Scintillation properties of Eu^{2+}-activated barium fluoroiodide

Gautam Gundiah,[1,*] Edith Bourret-Courchesne,[2] Gregory Bizarri,[1] Stephen M. Hanrahan,[1] Anurag Chaudhry,[1,3] Andrew Canning,[4] William W. Moses[1] and Stephen E. Derenzo,[1]

[1] *Life Sciences Division, Lawrence Berkeley National Laboratory, Berkeley, CA 94720, USA*

[2] *Materials Sciences Division, Lawrence Berkeley National Laboratory, Berkeley, CA 94720, USA*

[3] *Department of Electrical and Computer Engineering, University of California, Davis, CA 95616*

[4] *Computational Research Division, Lawrence Berkeley National Laboratory, Berkeley, CA 94720*

Abstract

The scintillation properties of powders and single-crystals of BaFI doped with Eu^{2+} are presented. Single crystals were grown by the vertical Bridgman technique. Under optical and X-ray excitation, the samples exhibit a narrow Eu^{2+} *5d-4f* transition emission centered at 405 nm. The scintillation light output is estimated to be 55,000±5,000 photons/MeV at 662 keV with 85% of the light decaying within 600 ns. An energy resolution of 8.5% full width at half maximum (FWHM) has been achieved using this scintillator for 662 keV excitation (^{137}Cs source) at room temperature.

Keywords—barium fluoroiodide, BaFI, europium, gamma-ray detection, scintillators.

* Corresponding author:

Email: GGundiah@lbl.gov; Tel. 1-510-486-5651; Fax. 510-486-4768

Introduction

Inorganic scintillators play an important role in the detection of ionizing radiation and find applications in national security, medical imaging as well as high-energy physics. Some critical requirements for these materials include high light yield (>20,000 photons per absorbed particle), fast response (below 1,000 ns), good energy resolution (<5% FWHM at 662 keV), high density (>4 g/cc) and good stopping power [1]. In addition, practical issues such as ease of crystal growth and moisture sensitivity play an important role in determining the application of these materials.

In the past decade, there has been significant attention devoted to Ce^{3+}-doped oxides and halides that show the electric dipole allowed $5d \rightarrow 4f$ transition [2-8]. Besides Ce^{3+}, $d \rightarrow f$ transitions are also observed in Eu^{2+}-doped compounds. The luminescence decay of Eu^{2+} (hundreds of nanoseconds) is much slower than that of Ce^{3+} (tens of nanoseconds), but still fast enough for many applications, especially those that do not require good timing resolution of high counting rates, such as national security. As early as 1968, Hofstadter reported the scintillation properties of SrI_2:Eu single crystals [9]. Cherepy *et al*. [10] revisited SrI_2:Eu to obtain a light output of 90,000 photons/MeV with an energy resolution of 4% FWHM at 662 keV and showing excellent proportionality. More recently, there have been reports of several bright Eu^{2+} activated halide scintillators [11,12].

In our quest for Eu^{2+} scintillators, we have investigated the mixed halide system barium fluoroiodide, BaFI. In the 1980's, Fuji developed BaFI:Eu^{2+} as a photostimulable X-ray phosphor for computed tomography [13]. We have performed first principle electronic structure calculations for Eu-doped BaFI to show that there is a localized excited state electron of Eu *5d* character below the conduction band of the host, which is necessary for efficient scintillation. Samples of BaFI:Eu^{2+} were synthesized as powders as well as single crystals using the vertical Bridgman technique. The structure was characterized using X-ray diffraction (XRD) and the luminescence using optical, X-ray and gamma-ray excitation. Presented below are the results of the investigation.

Experimental procedure

Synthesis:

Powders with the general composition $Ba_{1-x}Eu_xFI$ (x=0-0.5) were obtained by a solid state route using the respective halides as precursors. High-purity reactants were obtained from Sigma-Aldrich and used without further purification. Stoichiometric amounts of BaF_2, BaI_2, EuF_2 and EuI_2 were thoroughly mixed by dry grinding in an agate mortar and pestle in an Ar filled glove-box. The powders were sealed in an evacuated quartz tube and heated to 700 ^oC for 10h to yield the desired product. The reaction could also be performed by heating the reactants in an alumina crucible to 725 ^oC for 10h in flowing Ar-H_2 gas.

BaFI melts congruently at 900 ^{o}C and we have used the vertical, melt-based Bridgman technique to grow single crystals in sealed carbon-coated quartz tubes. The temperature gradient was about 30^{o}C/cm and the growth rate 1mm/h.

Characterization:

A detailed description of the high-throughput setup used for characterizing the samples is presented in [14]. The purity of the samples was confirmed using powder X-ray diffraction (XRD) with a Bruker Nonius FR591 rotating anode X-ray generator equipped with a copper target and a 50 kV and 60 mA electron beam. The crystal structure visualization Diamond was used to view the crystal structure. X-ray excited emission spectra were measured at the second port of the Bruker Nonius x-ray generator and their spectral response was recorded by a SpectraPro-2150i spectrometer (Acton Research Corp., Acton, MA) coupled to a PIXIS:100B charge-coupled detector (Princeton Instruments, Inc., Trenton, NJ). Photoluminescence (PL) excitation and emission spectra were measured at room temperature utilizing a Horiba Fluorolog 3 fluorescence spectrometer within the spectral range of 250 nm–800 nm. The X-ray excited decay curves were measured on a custom made pulsed X-ray system consisting of an ultrafast laser (200 fs pulses at 165 kHz), a light-excited X-ray tube, a Hamamatsu R3809U-50 microchannel PMT, and an Ortec 9308 picosecond time analyzer. The impulse response of the system is 100 ps FWHM. Pulse height spectra were recorded under gamma-ray excitation (^{137}Cs) with a Hamamatsu R6231-100 photomultiplier tube (PMT) connected to an Ortec 113 preamplifier, an Ortec 672 spectroscopic amplifier and an Ortec EASY-MCA-8K multichannel analyzer. The PMT high voltage was fixed at 650 V. Samples were optically coupled onto the window of the PMT with Viscasil 600000 (GE) and covered with layers of ultraviolet light reflecting tape (PTFE).

First principles calculations:

First principles calculations of Eu-doped BaFI were carried out using the generalized gradient approximation to density functional theory as implemented in the VASP code [15,16] using PAW pseudopotentials [17]. An on-site correction for the Eu 4f electrons was applied using the LSDA+U implementation of Dudarev et al. [18]. The ground state of the Eu-doped compound is calculated by substituting a single Eu^{2+} impurity ion on a Ba^{2+} site and then relaxing the atomic positions at fixed cell volume. The forces on all atoms in every direction are less than 0.01 eV/A in the relaxed geometry. A ground state calculation showed that the Eu *4f* states were above the valence band.

Results and discussion

Structural characterization:

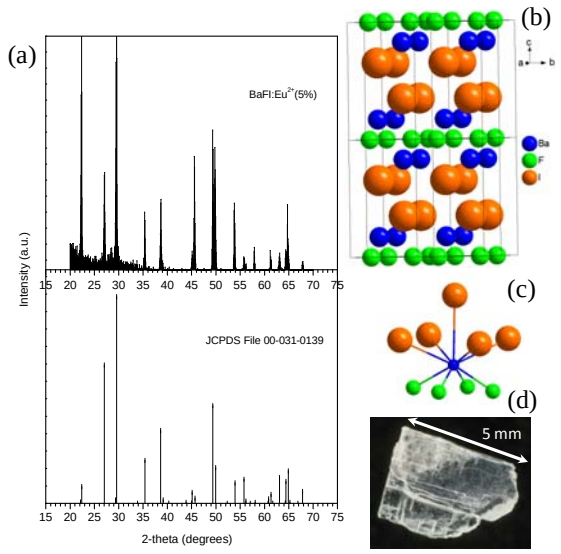

Figure 1: (a) XRD pattern for BaFI:Eu(5%) as compared to the JCPDS standard pattern. (b) Schematic of the crystal structure of BaFI with (c) the environment around single Ba atoms. Atoms in blue represent Ba/Eu, green F and orange I atoms. (d) Photograph of a single crystal with length ~5 mm.

The products are not sensitive to moisture and can be handled under ambient conditions. While the crystals are transparent, the powders are cream colored. BaFI has a tetragonal structure analogous to the matlockite (PbFCl) structure with a density of 5 g/cm^3. The XRD pattern (Figure 1(a)) showed the characteristic peaks of BaFI with no impurities corresponding to reactants or dopant. Based on size and charge considerations, the dopant Eu (ionic radius 1.30 Å) is expected to replace Ba (ionic radius 1.47 Å) in the lattice [19]. The structure, shown in Figure 1(b), consists of layers of halogen, due to which it is fairly easy to cleave the crystals perpendicular on the c axis and might make it challenging to grow and handle crystals with thickness in the centimeter range. The structure contains a single site for Ba/Eu located at the center of a square antiprism, surrounded by 4F and 5I atoms (Figure 1(c)). The crystals used in this study were plate-like with a width between 2-5 mm and a thickness between 0.1-1 mm. We show a photograph of a crystal in Figure 1(d).

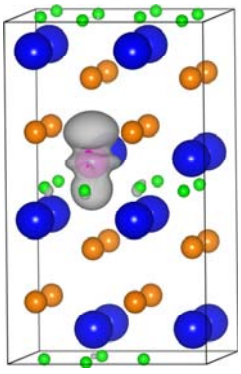

Figure 2: Isosurface of the electron density for the (Eu^{2+})* excited state of BaFI:Eu showing strong localization on the Eu atom (pink), Ba (blue), F (green), I (orange). Calculations were performed with the VASP code.

First principles calculations:

Excited state calculations for the $(Eu^{2+})^*$ ([Xe]$4f^6 5d^1$) state, were carried out by setting the occupancy of the seventh highest Eu *4f* state to zero. Figure 2 shows the isosurface of electron density for the $(Eu^{2+})^*$ state. This excited state is extremely localized on the Eu site, is of *5d* character and lies below the conduction band of the host material favoring a *5d-4f* type transition. Details of this approach for excited state calculations of Ce doped systems were presented in reference [20].

The main goal of our calculations is to show that there is a localized excited state of Eu *5d* character below the host conduction band and a *4f* character state above the valence band. This indicates that a *5d-4f* transition is very likely to occur assuming the energy transfer mechanism from the host to the Eu site is efficient.

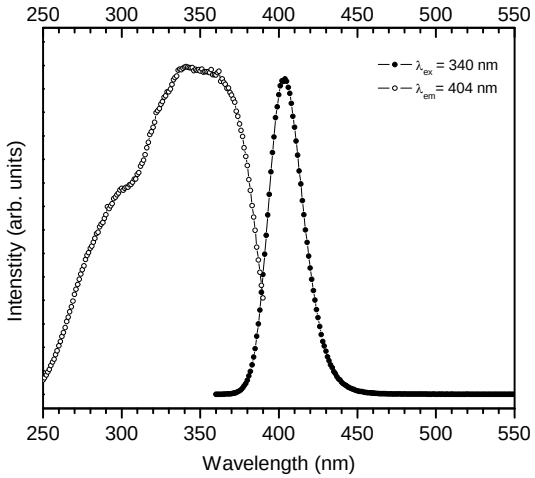

Figure 3: Room temperature excitation (left) and emission (right) curves for BaFI:Eu^{2+} powders.

Photoluminescence properties:

Room temperature excitation and emission curves are shown in Figure 3. The emission consists of a single peak centered at 404 nm with a FWHM of 20 nm. We attribute the single emission peak to the $4f^6 5d^1 \rightarrow 4f^7$ transition of Eu^{2+}. The excitation spectrum consists of a broad, featureless band between 260 and 370 nm. On excitation in this region, we observe the 404 nm Eu^{2+} emission. The single emission is consistent with the presence of a single site for Eu in the lattice.

Scintillation properties:

Figure 4 shows the normalized X-ray excited emission spectra for BaFI doped with different amount of Eu recorded at room temperature. The undoped sample shows a broad emission from the host centered around 490 nm. On adding 1% Eu dopant, we observe that the spectrum is

dominated by a narrower emission at 404 nm in addition to the weak host emission. The position

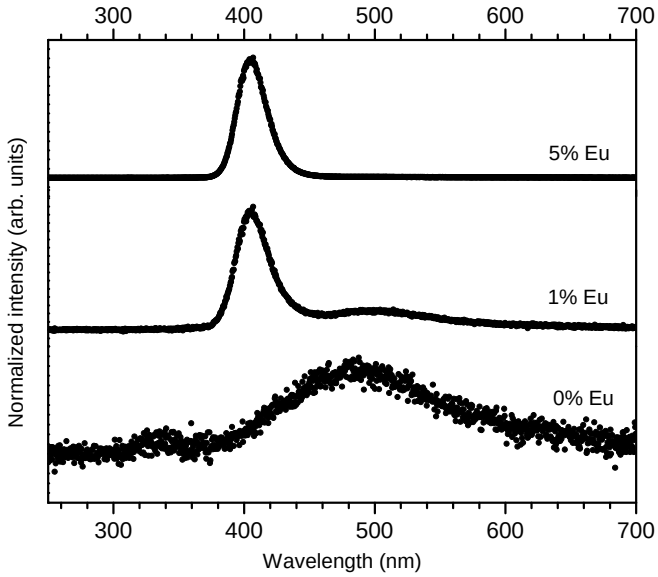

Figure 4: Variation of X-ray luminescence of BaFI powders.

of the emission is similar to the optical emission as well as literature reports on BaFI:Eu^{2+} powders [13] and is attributed to the characteristic *5d-4f* transition of Eu^{2+}. On increasing the amount of Eu to 5%, the host emission totally disappears and we observe the single emitting center centered at 404 nm. Thus, the absorbed energy is efficiently transferred to the dopant europium ions. The optimal dopant concentration was determined to be 5%.

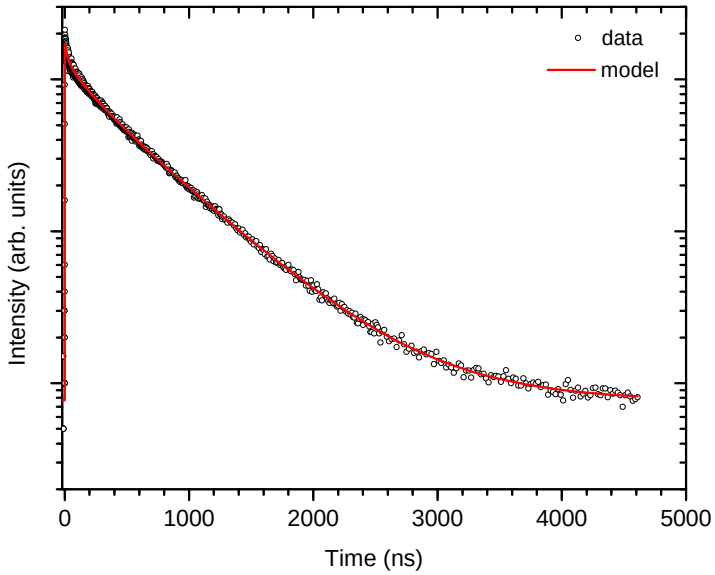

Figure 5: Room temperature pulsed X-ray decay curve of BaFI:Eu (5%) single crystal.

Figure 5 shows the X-ray excited decay curve of a BaFI:Eu^{2+} (5%) single crystal. The decay curve exhibits three single exponential components with lifetimes 163, 573 and 905 ns. The

decay is dominated by 573 ns component that accounts for 81% of the light, while the remaining components account for 7 and 6% respectively.

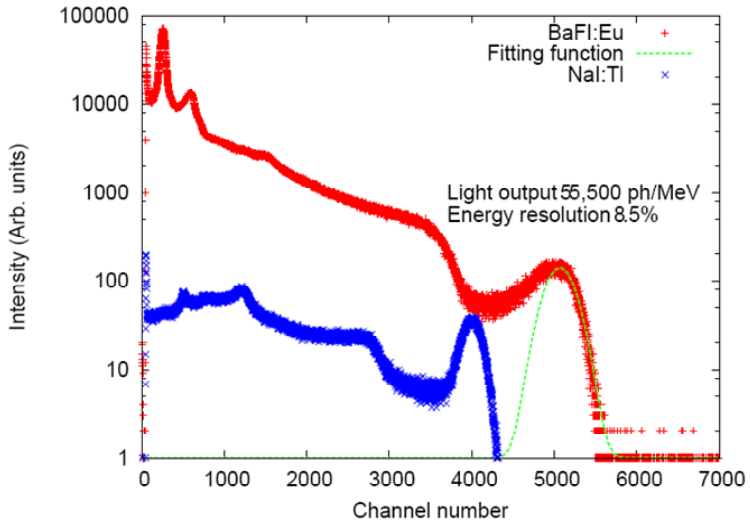

Figure 6: Pulsed height spectra of BaFI:Eu and NaI:Tl single crystals measured under 137Cs (662 keV) gamma ray.

Presented in Figure 6 is the pulse height spectrum for BaFI:Eu^{2+} and NaI:Tl^{+} (S. Gobain) under ^{137}Cs irradiation (662 keV) and amplifier shaping time of 10 µs. The BaFI crystal used in the study has a width of ~2 mm and thickness of ~0.3 mm. The spectrum for BaFI:Eu consists of the photopeak (centered approximately at channel number 5000), the Compton edge (approximately at channel number 3500), the backscattered peak (approximately at channel number 1300) and the Ba-escape peak (approximately at channel number 200). Similar features are observed in the spectrum of the NaI:Tl crystal. For both the crystals, the Compton-photopeak distance was identical to the backscattered peak-zero distance, thus indicating that the signal was not saturated. The feature approximately at channel number 500 could be attributed to being from gamma rays scattered by the surroundings in the experimental setup. To determine the photopeak position and energy resolution of the crystals, part of the photopeak was fitted by Gaussian curves. The region of the peak between channel number 4000 and 4600 could be the X-ray escape peak that is present due to several factors such as the small size of the crystal, the poor crystal quality or in-scattering from the surroundings. The light output was estimated by comparison with the response of NaI:Tl (cylindrical with a diameter of 1 inch and height 1 inch) that has a luminosity between 43,000 and 45,000 ph/MeV [21,22]. The light output for BaFI:Eu was estimated to be 55,000 ± 5,000 ph/MeV. The energy resolution is defined as the FWHM of the 662 keV full absorption peak. A value of 8.5% was measured. Luminosity values for some scintillators have been found to decrease with increasing crystal size [23]. Since the NaI:Tl crystal used as a reference is significantly larger than our crystal, there is a possibility of overestimation of the luminosity value. Improvements in the crystal quality are expected to improve the light yield and energy resolution.

Conclusion

We have described the synthesis and scintillation properties of Eu^{2+}-activated BaFI. Single-crystals were grown by the Bridgman technique. On irradiation with 662 keV, the estimated light yield was 55,000 ph/MeV and the energy resolution 8.5%. ~85% of the light decayed within 600 ns. While the scintillation properties and moisture-resistant nature are encouraging, growth of large sized crystals due to the layered structure could be challenging.

Acknowledgment

The authors thank Marvin Weber, Yetta Eagleman, Ramesh Borade and Zewu Yan for useful discussions and invaluable suggestions. This work was supported by the U.S. Department of Homeland Security/DNDO and the U.S. Department of Energy/NNSA/NA22 and carried out at Lawrence Berkeley National Laboratory under Contract NO. AC02-05CH11231.

References

[1] P. A. Rodnyi, *Physical Processes in Inorganic Scintillators*, CRC Press, Boca Raton, FL, 1997.

[2] M. J. Weber, "Inorganic scintillators: today and tomorrow," *J. Lumin.*, vol. 100, pp. 35-45, 2002.

[3] E. V. D. van Loef, P. Dorenbos, C. W. E van Eijk, K. Krämer and H. U. Güdel, "High-energy-resolution scintillator: Ce^{3+} activated $LaCl_3$," *Appl. Phys. Lett.*, vol. 77, pp. 1467-1468, 2000.

[4] E. V. D. van Loef, P. Dorenbos, C. W. E van Eijk, K. Krämer and H. U. Güdel, "High-energy-resolution scintillator: Ce^{3+} activated $LaBr_3$," *Appl. Phys. Lett.*, vol. 79, pp. 1573-1575, 2001.

[5] O. Guillot-Noel, J. T. M. de Haas, P. Dorenbos, C. W. E. van Eijk, K. Krämer and H. U. Güdel, "Optical and scintillation properties of cerium-doped $LaCl_3$, $LuBr_3$ and $LuCl_3$," *J. Lumin.*, vol. 85, pp. 21-35.

[6] R. Hawrami, A. K. Batra, M D. Aggarwal, U. N. Roy, M. Groza, Y. Cui, A. Burger, N. Cherepy, T. Niedermayr and S. A. Payne, "New scintillator materials (K_2CeBr_5 and Cs_2CeBr_5)," *J. Cryst. Growth*, vol. 310, pp. 2099-2102, 2008.

[7] Y. D. Porter-Chapman, E. D. Bourret-Courchesne, G. A. Bizarri, M. J. Weber and S. E. Derenzo, "Scintillation and Luminescence Properties of Undoped and Cerium-Doped $LiGdCl_4$ and $NaGdCl_4$," *IEEE Trans. Nucl. Sci.*, vol. 56, pp. 881-886, 2009.

[8] P. A. Rodnyi, V. B. Mikhailik, G. B. Stryganyuk, A. S. Voloshinovskii, C. W. E. van Eijk, G. F. Zimmerer, "Luminescence properties of Ce-doped $Cs_2LiLaCl_6$ crystals," *J. Lumin.*, vol. 86, pp. 161-166, 2000.

[9] R. Hofstandter, "Europium activated strontium iodide scintillators," US Patent 3,373,279, March 12, 1968.

[10] N. J. Cherepy, G. Hull, A. D. Drobshoff, S. A Payne, E. van Loef, C. M. Wilson, K. S. Shah, U. N. Roy, A. Burger, L. A. Boatner, W.-S. Choong, W. W. Moses, "Strontium and barium iodide high light yield scintillators," *Appl. Phys. Lett.*, vol. 92, 083508.1-083508.3, 2008.

[11] E. D. Bourret-Courchesne, G. Bizarri, R. Borade, Z. Yan, S. M. Hanrahan, G. Gundiah, A. Chaudhry, A. Canning and S. E. Derenzo, "Eu^{2+}-doped Ba_2CsI_5, a new high-performance scintillator," *Nucl. Instru. Met. A*, 2009, accepted.

[12] E. D. Bourret-Courchesne, G. Bizarri, S. M. Hanrahan, G. Gundiah, Z. Yan and S. E. Derenzo, "BaBrI:Eu^{2+}, a new bright scintillator," *Nucl. Instru. Met. A*, 2009, accepted.

[13] M. Sonoda, M. Takano, J. Miyahara and H. Kato, "Computed Radiography Utilizing Scanning Laser Stimulated Luminescence," *Radiology*, vol. 148, pp. 833-838, 1983.

[14] S. E. Derenzo, M. Boswell, E. Bourret-Courchesne, R. Boutchko, T. F. Budinger, A. Canning, S. M. Hanrahan, M. Janecek, Q. Peng, Y. Porter-Chapman, J. Powell, C. A. Ramsey, S. E. Taylor, L.-W. Wang, M. J. Weber and D. S. Wilson, "Design and implementation of a facility for discovering new scintillator materials," *IEEE Trans. Nucl. Sci.*, vol. 55, pp. 1458-1463, 2008.

[15] G. Kresse and J. Hafner, "Abinitio molecular-dynamics for liquid-metals," *Phys. Rev. B*, vol. 47, pp. 558-561, 1993.

[16] G. Kresse and J. Furthmuller, “Efficient iterative schemes for ab initio total-energy calculations using a plane-wave basis set,” *Phys. Rev. B*, vol. 54, pp. 11169-11186, 1996.

[17] G. Kresse and D. Joubert, “From ultrasoft pseudopotentials to the projector augmented-wave method,” *Phys. Rev. B*, vol. 59, 1758-1775, 1999.

[18] S. L. Dudarev, G. A. Botton, S. Y. Savrasov, C. J. Humphreys, and A. P. Sutton, “Electron-energy-loss spectra and the structural stability of nickel oxide: An LSDA+U study,” *Phys. Rev. B*, vol. 57, pp. 1505-1509, 1998.

[19] R. D. Shannon and C. T. Prewitt, “Effective ionic radii in oxides and fluorides,” *Acta Cryst.*, vol. B25, pp. 925-946, 1969.

[20] A. Canning, R. Boutchko, A. Chaudhry, and S. E. Derenzo, “First-principles studies and predictions of Scintillation in Ce-doped materials,” *IEEE Transactions on Nuclear Science*, vol. 53, pp. 944-948, 2009

[21] E. Sakai, “Recent measurements on scintillator-photodetector systems,” *IEEE Trans. Nucl. Sci*., vol. 34, pp. 418-422, 1987.

[22] I. Holl, E. Lorenz and G. Mageras, “A measurement of the light yield of common inorganic scintillators,” *IEEE Trans. Nucl. Sci.*, vol. 35, pp. 105-109, 1998.

[23] W. Drozdowski, P. Dorenbos, A. J. J. Bos, J. T. M. de Haas, S. Kraft, E. Maddox, A. Owens, F. G. A. Quarati, C. Dathy and V. Ouspenski, “Effect of proton dose, crystal size, and cerium concentration on scintillation yield and energy resolution of $LaBr_3$:Ce,” *IEEE Trans. Nucl. Sci.*, vol. 54, pp. 736-740, 2007.